MODELING FUNCTIONALLY GRADED INTERPHASE REGIONS IN CARBON NANOTUBE REINFORCED COMPOSITES

G. D. Seidel, D. C. Lagoudas

Department of Aerospace Engineering,

Texas A&M University, College Station, TX 77843-3141

S. J. V. Frankland

National Institute of Aerospace

100 Exploration Way, Hampton, VA 23666

T. S. Gates

NASA Langley Research Center, Hampton, VA 23681

ABSTRACT

A combination of micromechanics methods and molecular dynamics simulations are used to obtain the effective properties of the carbon nanotube reinforced composites with functionally graded interphase regions. The multilayer composite cylinders method accounts for the effects of non-perfect load transfer in carbon nanotube reinforced polymer matrix composites using a piecewise functionally graded interphase. The functional form of the properties in the interphase region, as well as the interphase thickness, is derived from molecular dynamics simulations of carbon nanotubes in a polymer matrix. Results indicate that the functional form of the interphase can have a significant effect on all the effective elastic constants except for the effective axial modulus for which no noticeable effects are evident.

INTRODUCTION

Carbon nanotube reinforced polymer composites are attracting much interest as multifunctional materials. Two key issues which have emerged in such composites are the adequate dispersion of carbon nanotubes within the polymer matrix and good adhesion between the carbon nanotubes and surrounding matrix. Efforts to address both issues from a processing point of view have identified chemical functionalization of carbon nanotubes as one solution, leading to an increased importance of the interphase region between carbon nanotubes and the surrounding matrix. Differing

forms of carbon nanotube functionalization affect both interphase thickness and how the material properties within the interphase vary through the thickness. The interphase region in these composites can therefore be modeled as a functionally graded material.

Recently, molecular dynamics simulations have revealed the presence of a functionally graded interphase even in non-functionalized carbon nanotube reinforced polymer matrix composites [1,2]. This interphase is the region in which the local density of the polymer varies from the bulk density. Because it involves a representation of the atomistic structure, molecular dynamics simulation is well-suited to predicting properties at this local scale. In the molecular dynamics simulations, the density variation can be determined from the molecular structure of the polymer chains packing around the nanotube. This information can then be used in the multi-layered composite cylinders model [3] to examine the effect of the interphase on the elastic properties of carbon nanotube reinforced composites. A multi-scale model can, therefore, be established, which utilizes the atomistic details from the MD and incorporates them into the micromechanical model.

In the present work, the multi-layered composite cylinders model [3] is used to model a functionally graded interphase region with an increasing number of piecewise continuous subregions. The objective is to obtain the effective elastic constants of carbon nanotube reinforced composites from the micromechanical model, but to refine the number and properties of the subregions to approximate the density variations observed in the molecular structure.

The first section of this paper discusses the molecular dynamics simulations of a carbon nanotube in a polyethylene matrix used to determine the radial distribution in density. The subsequent section discusses the multi-layered composite cylinders micromechanics model used to obtain effective continuum level elastic constants. The Results and Discussion section provides the details of how the molecular dynamics radial density distribution motivated the selection of number, size, and stiffness of interphase regions in the micromechanics analysis. Also in that section, effective axial modulus, axial Poisson's ratio, axial shear modulus and in-plane bulk modulus results obtained from the multi-layered composite cylinders solution over the applicable range of volume fractions are provided.

MOLECULAR DYNAMICS SIMULATIONS

The molecular structure of the polymer nanotube composite in Figure 1 was generated with molecular dynamics simulation and is from the simulations in References [1] and [2]. The polymer is polyethylene and is composed of 8 chains of 1095 $-CH_2-$ (methylene) units. The nanotube is a (10,10) single-walled carbon nanotube of radius 6.78 A with 1,720 C-atoms. The simulation box is approximately 5x5x10 nm where the nanotube is 10 nm in length, and as such, corresponds to a volume fraction (based on the outer radius of the carbon nanotube) of approximately 10%. The polymer and the nanotube were modeled with the many-body bond-order potential developed by Brenner, et al. [4]. The interaction between the polyethylene and the nanotube was represented with the Lennard-Jones potential.

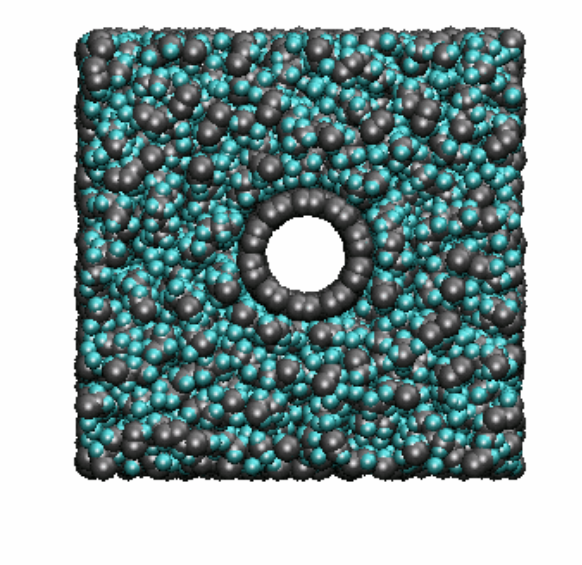

Figure 1. Top view of the molecular dynamics simulation box of a carbon nanotube in a polyethylene matrix. Carbon atoms, both in the carbon nanotube and in the polyethylene, are depicted as dark sphere and hydrogen atoms as lighter spheres (carbon and hydrogen atoms are not to scale). The simulation box is approximately 5x5x10 nm.

In Figure 2 the density of the system relative to bulk polymer density is plotted as a function of the radial distance from the nanotube center. The average structural data is plotted for one configuration from the simulation trajectory. The first peak between 6 and 7 A is from the atoms of the carbon nanotube wall. The second peak at 11 A is the first polymer peak which is enhanced at 1.5 times the bulk polymer density (normalized to 1 in this plot).

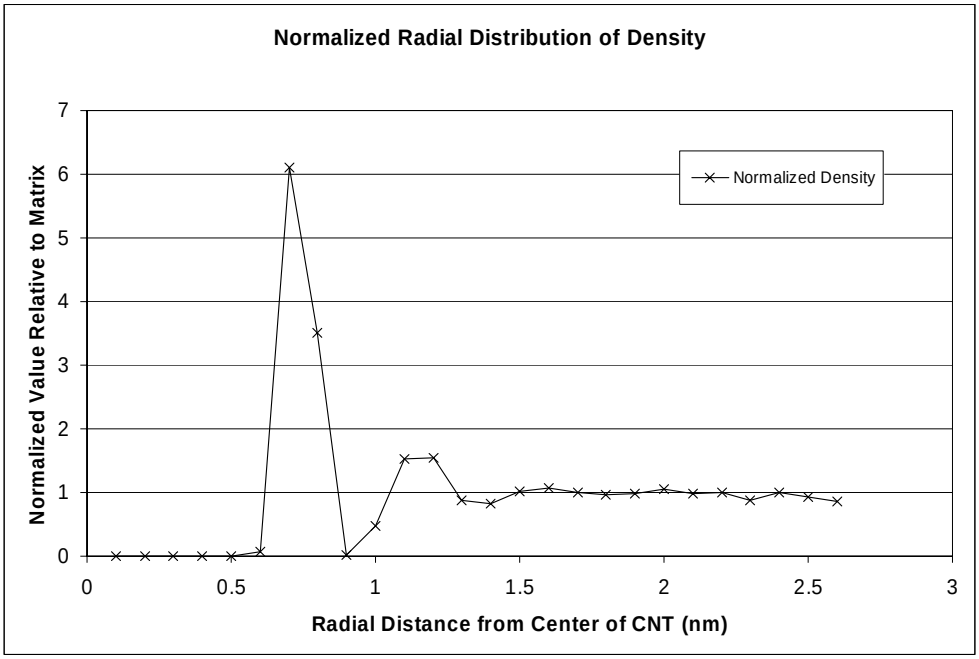

Figure 2. Radial distribution of density normalized by the bulk density of polyethylene measured from the carbon nanotube center.

The normalized density data after the carbon nanotube spike is indicative of a functionally graded interphase region ranging from approximately 0.85 nm to 1.5 nm which provides the motivation for micromechanics modeling which follows.

MULTI-LAYERED COMPOSITE CYLINDERS MODEL

The multi-layered composite cylinder model employed herein is based on the earlier works of Hashin and Rosen [5] and Christensen and Lo [6], and is discussed in detail in Reference [3]. A brief description of the model is provided here. Figure 3 provides a schematic of the composite cylinder assemblage for a multi-layered composite cylinder. The innermost phase, Phase 1, corresponds to the fiber, in this case the carbon nanotube. Herein, the non-hollow portion of the nanotubes are considered to be isotropic linear elastic with material properties corresponding to the in-plane properties of graphite, i.e. Young's modulus of 1.1 TPa and Poisson's ratio of 0.14. The outermost phase, Phase N, corresponds to the matrix, which for the present work is polyethylene. The bulk polyethylene properties used in the present study correspond to medium density polyethylene with a Young's modulus of 0.46 GPa and Poisson's ratio of 0.38 [7]. Any region of non-zero thickness between Phases N and 1 is considered to be an interphase region which, based on the molecular dynamics simulations, should be a functionally graded region. Thus, for a single interphase region, N would be equal to three. In the present study, the functionally graded nature of the interphase region is treated using multiple piecewise continuous interphase regions so that N is equal to the number of piecewise continuous regions plus two. It

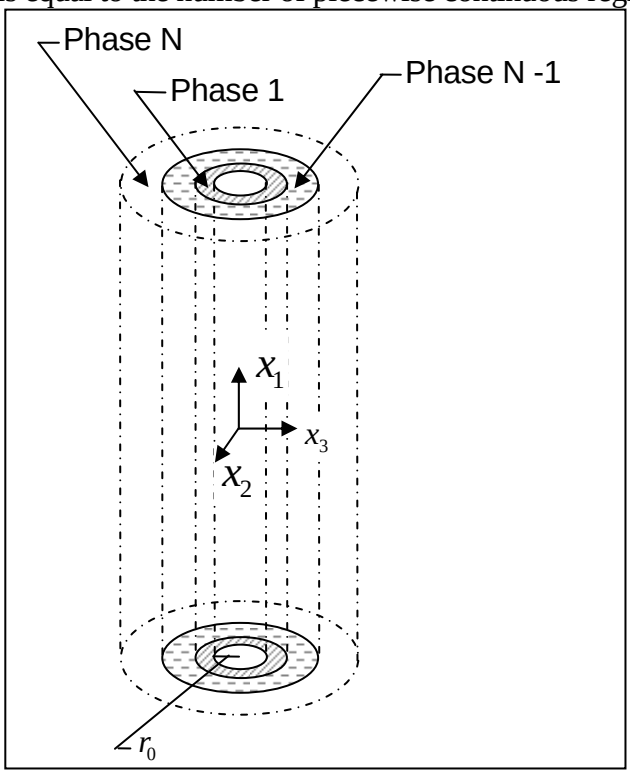

Figure 3. Multi-layered composite cylinders assemblage. Phase 1 corresponds to the carbon nanotube and Phase N to the polyethylene matrix. Intermediate phases are considered to be interphase regions.

should be noted that the hollow and non-hollow portions of the nanotube are considered to be a single phase in description only. Effective properties for the composite cylinders assemblages are calculated with boundary conditions of zero traction applied to the inner surface of the nanotube to accurately account for the zero stiffness hollow region.

In addition to knowing the elastic constants for each phase, the relative size of each phase must be identified. The inner and outer radii of Phase 1 are identified as r_0 and r_1, respectively. The outer radius of Phase N, r_N, is determined by the desired volume fraction, c_f, of Phase 1 using Equation 1. The inner radius of the N^{th} Phase is determined by the presence, or lack thereof, of an interphase region and its thickness. If no interphase is present, then the inner radius of Phase N is r_1. If there is an interphase of thickness t, then a critical volume fraction, c_{cr}, can be identified at which r_N becomes the outer radius of the last interphase region, r_{N-1} ($r_{N-1} = r_1 + t$ for a single interphase). At this volume fraction, the concentration of nanotubes is such that the outermost interphase region surrounding the nanotubes would be in contact. This critical volume fraction is given by Equation 2, and represents a limit in applicability of the composite cylinders assemblage shown in Figure 3 as at higher volume fractions, the interphase would no longer be cylindrical and the matrix phase would no longer completely envelope the nanotube and its interphase(s). Thus, results contained herein are shown for volume fractions up to the critical volume fraction.

$$r_N = \frac{r_1}{\sqrt{c_f}} \tag{1}$$

$$c_{cr} = \frac{r_1^2}{r_{N-1}^2} \tag{2}$$

To briefly illustrate the micromechanics modeling approach, the relevant equations for determining the effective in-plane bulk modulus are summarized here. The displacement field corresponding to an in-plane bulk test for a homogenous material given in Equation 3 is assumed for each phase one through N, were the B_1^i and B_2^i are constants to be determined through the boundary and matching conditions in Equations 4 and 5, respectively. The boundary condition expressed in Equation 4a corresponds to a traction free surface on the interior of the nanotube. Equation 5a and 5b denote the continuity of displacements and tractions, respectively, across the interfaces of neighboring phases (here interface denotes an internal phase boundary). Equations 4 and 5 represent 2N equations which, using the linearized strain-displacement relations and the constitutive equations for each phase (all phases are isotropic linear elastic), are used to solve for the 2N unknown constants, B_1^i and B_2^i.

$$\begin{aligned} u_r^i &= B_1^i r + \frac{B_2^i}{r} \quad \text{for } r_{i-1} \le r \le r_i \text{ and } i = 1..N \\ u_\theta^i &= u_z^i = 0 \end{aligned} \tag{3}$$

$$\sigma_{rr}^{1} = 0 \text{ at } r = r_0 \tag{4a}$$

$$u_r^N = \varepsilon_0 r_N \text{ at } r = r_N \tag{4b}$$

$$u_r^j = u_r^{j+1} \text{ at } r = r_j \text{ and } j = 1..N-1 \tag{5a}$$

$$\sigma_{rr}^j = \sigma_{rr}^{j+1} \text{ at } r = r_j \text{ and } j = 1..N-1 \tag{5b}$$

The effective in-plane bulk modulus is then determined through the strain energy equivalence between the composite cylinders assemblage and a homogeneous transversely isotropic cylinder of radius r_N subject to the same displacement boundary conditions at r_N as the composite cylinder assemblage. It can be shown using the Hill-Mandel and divergence theorems that the strain energy equivalency can be expressed in terms of in-plane bulk modulus as shown in Equation 6 where the angled brackets denote volume averages. Similar procedures can be applied to obtain the effective axial modulus, axial Poisson's ratio, and axial shear modulus as discussed in Reference [3].

$$\kappa_{r\theta}^{eff} = \frac{\langle \sigma_{rr} \rangle}{2\langle \varepsilon_{rr} \rangle} = \left. \frac{\sigma_{rr}^N}{2\left(u_r^N / r_N\right)} \right| r = r_N \tag{6}$$

RESULTS AND DISCUSSION

Using Figure 2 as motivation, carbon nanotubes were assumed to have an inner radius of 0.51 nm and an outer radius of 0.85 nm, thus having a thickness of 0.34 nm consistent with the spacing of graphene sheets in graphite. Three cases were considered, one with no interphase, one with a single interphase, and one with two interphase regions, the total thickness of which is equal to the single interphase thickness. Based on the normalized density distribution in Figure 2, the region between the nanotube and the subsequent spike in density was considered to be very low density polyethylene (Young's modulus of 0.068 GPa [7]) while the spike itself was considered to be high density polyethylene (Young's modulus of 1.6 GPa [7]), both having the same Poisson's ratio as the medium density polyethylene matrix. Thus, for the two interphase case, the first interphase region was considered to be a 0.1 nm thick region of very low density polyethylene and the second region, a 0.2 nm thick region of high density polyethylene. For the single interphase case, the Young's modulus used was a weighted average of the two interphase case properties with a thickness of 0.3 nm. The normalized stiffness radial distribution for all three cases is provided in Figure 4 along with the normalized density distribution (minus the nanotube portion). A summary of the material properties and geometry of the composite cylinders assemblage is provided in Table I.

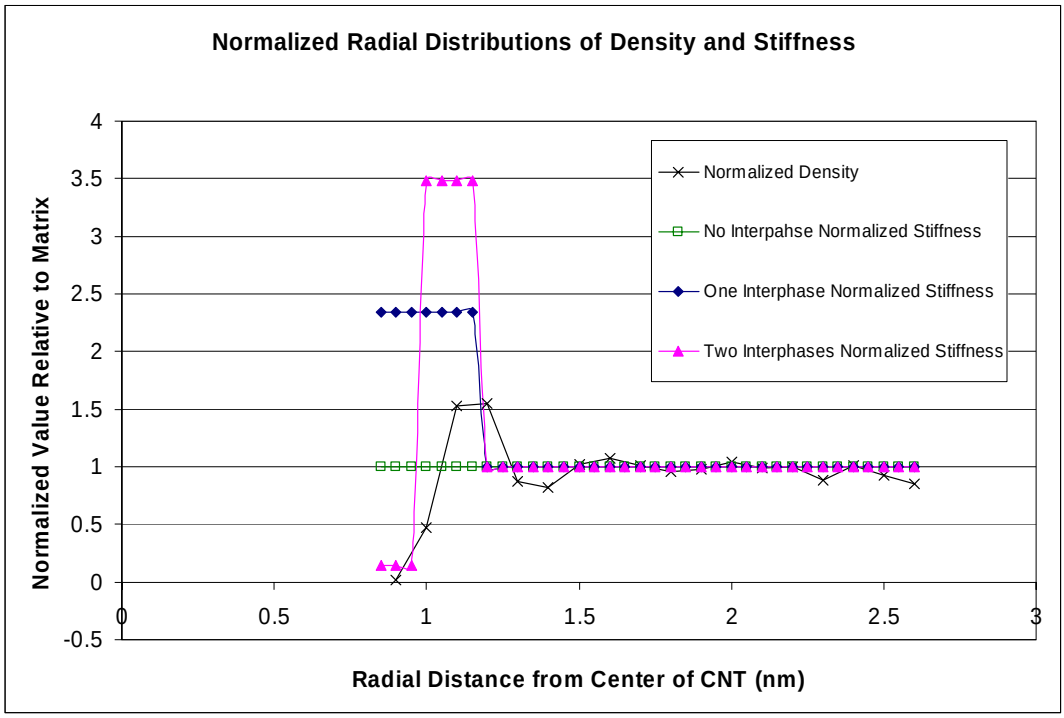

Figure 4. Radial density and stiffness distributions normalized by the corresponding matrix values. The density distribution is obtained from the molecular dynamics simulations.

Table I. Summary of composite cylinder assemblage geometry and material properties.

		Inner Radius (nm)	Outer Radius (nm)	Thickness (nm)	E (GPa)	υ
All Cases	Carbon Nanotube	0.51	0.85	0.34	1100	0.14
	Medium Density Polyethylene Matrix	r_{N-1}	r_N	r_N-r_{N-1}	0.46	0.38
Single Interphase	Interphase	0.85	1.15	0.3	1.079	0.38
Double Interphase	First Interphase	0.85	0.95	0.1	0.068	0.38
	Second Interphase	0.95	1.15	0.2	1.6	0.38

Figures 5 through 8 provide multi-layered composite cylinders results for the effective axial modulus, axial Poisson's ratio, axial shear modulus and in-plane bulk modulus for all three cases up to the critical carbon nanotube volume fraction of 54%. For the effective axial modulus, Figure 5 indicates that the presence of an interphase region has a negligible effect. This result is a consequence of the nanotubes carrying the majority of the applied axial load given the large stiffness of the nanotube and, consistent with the large aspect ratio of carbon nanotubes and the molecular dynamics simulations previously discussed, is a consequence of the neglecting of end effects in the multi-layered composite cylinders approach.

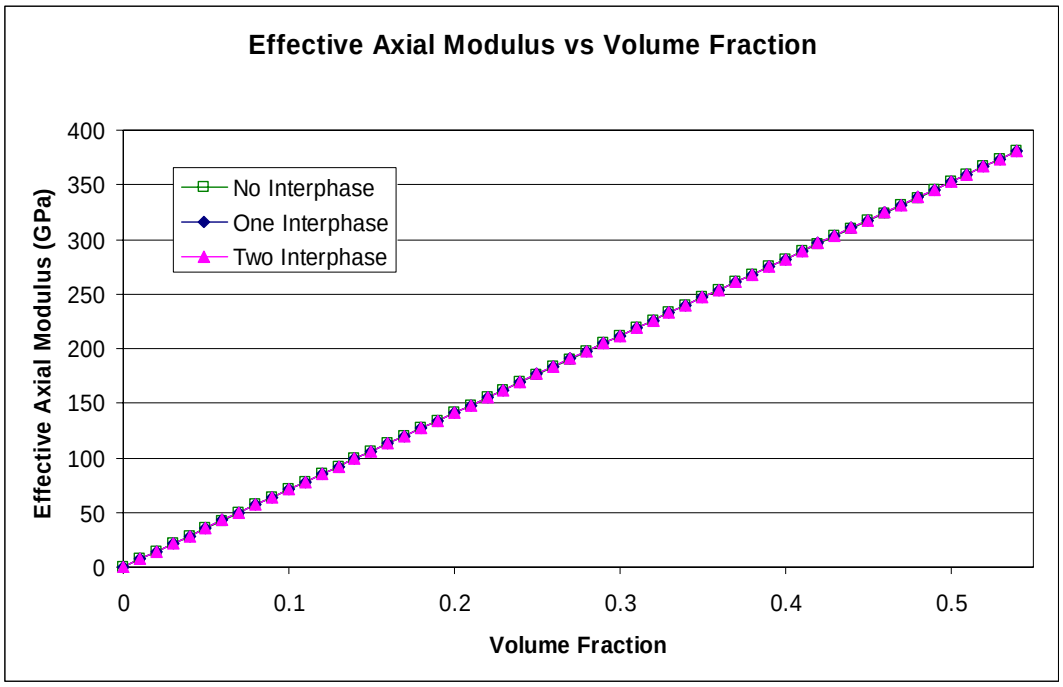

Figure 5. Multi-layered composite cylinder predictions of the effective axial modulus of carbon nanotube reinforced polyethylene.

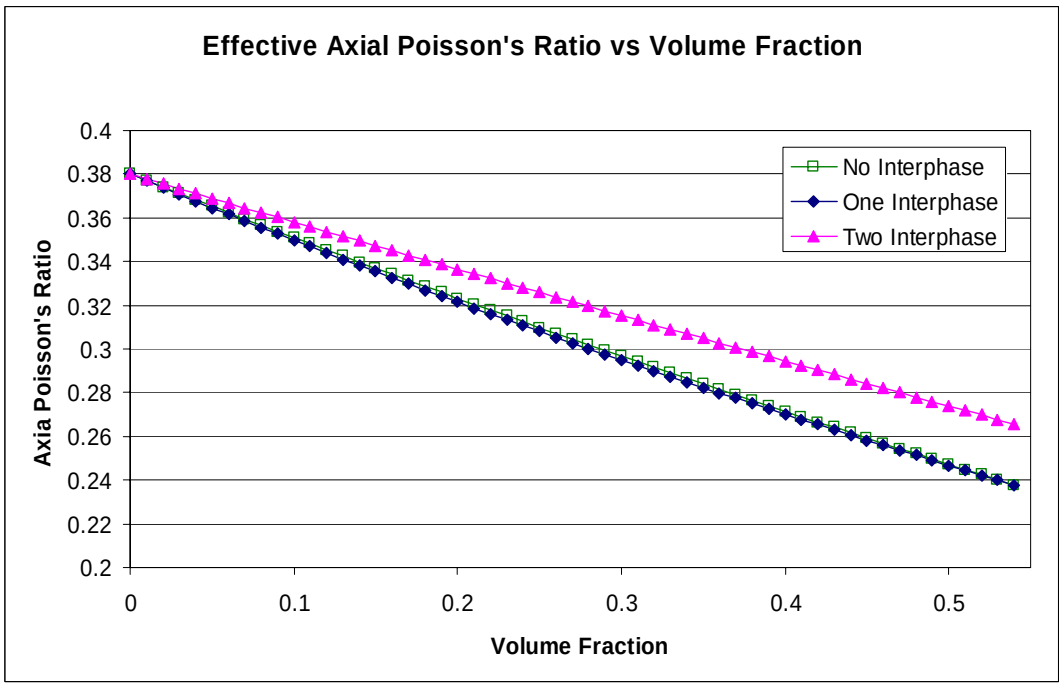

Figure 6. Multi-layered composite cylinder predictions of the effective axial Poisson's ratio of carbon nanotube reinforced polyethylene.

Despite having the same Poisson's ratio for the matrix and interphase regions in all three cases, the effective Poisson's ratio, as shown in Figure 6, does demonstrate a measurable effect as a result of the inclusion of interphase regions, in particular for the two interphase case. In the two interphase case, the compliance of the first interphase being greater than that of the matrix allows for greater radial contraction during the axial extension used to determine the effective axial modulus and Poisson's ratio. In contrast, the single interphase case has an interphase stiffness greater than that of the matrix, but still far less than the nanotube so that any additional resistance to radial contraction is hardly noticeable.

The effective axial shear modulus and in-plane bulk modulus shown in Figures 7 and 8, respectively, also show measurable effects of the presence of interphase regions. In fact, both properties are seen to have identical trends to one another, but are quite different from the trends shown in Figure 6 for the effective Poisson's ratio. For the single interphase case, the effective axial shear modulus and in-plane bulk modulus are much larger than the corresponding no interphase values, while for the two interphase case they are much less. Despite having a second interphase region whose stiffness is greater than that of the single interphase case, the effective axial shear modulus and in-plane bulk modulus in the two interphase case are dominated by the compliant nature of the first interphase, thus indicating the importance of accurate representation of the interphase region.

Both the difference in trends seen between Figure 6 and Figures 7 and 8 and the dominance of the first interphase region in the two interphase case is perhaps best explained by considering the effective in-plane bulk modulus. Recall that the radial contraction used to calculate the effective Poisson's ratio occurs under zero radial stress and is a measure of strain ratios. Thus, the amount of radial contraction between the one and two interphase cases can be quite different. However, as

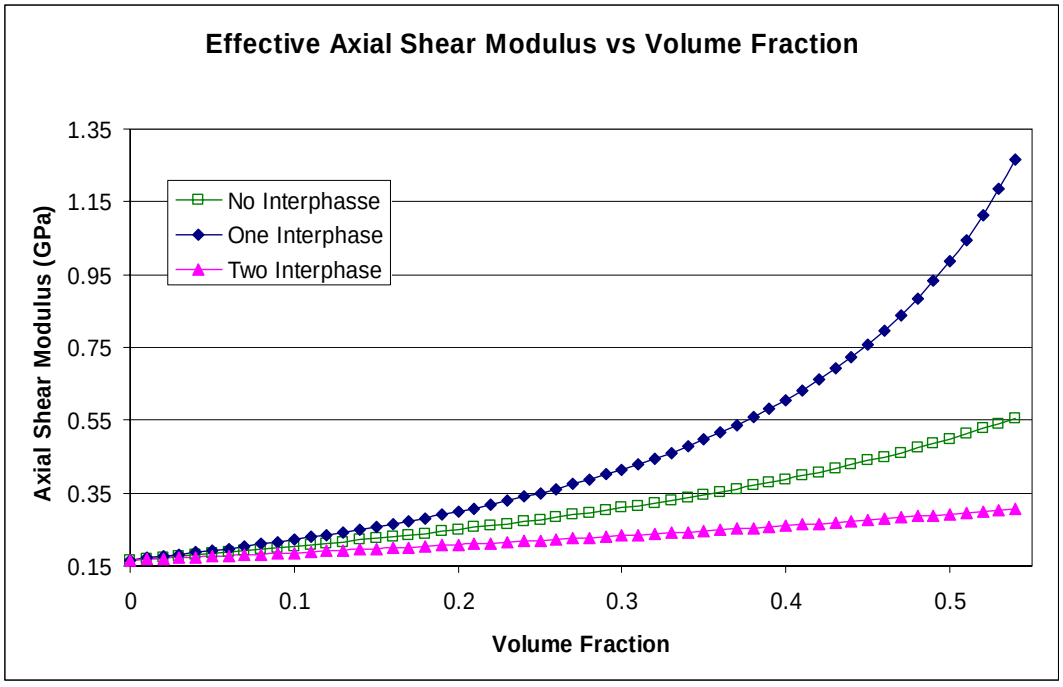

Figure 7. Multi-layered composite cylinder predictions of the effective axial shear modulus of carbon nanotube reinforced polyethylene.

indicated in Equation 6, the in-plane bulk modulus depends on both radial strain and stress. With all three cases having the same imposed displacement given in Equation 4b, all three cases have the same average radial strain. Thus it is the average radial stress which governs the differences seen in each case. The compliant nature of the first interphase in the two interphase case results in a lower average stress relative to the no interphase case as a disproportionately large amount of strain occurs in this region with little resulting stress. In the single interphase case, the interphase is stiffer than the matrix and thus elevates the average radial stress.

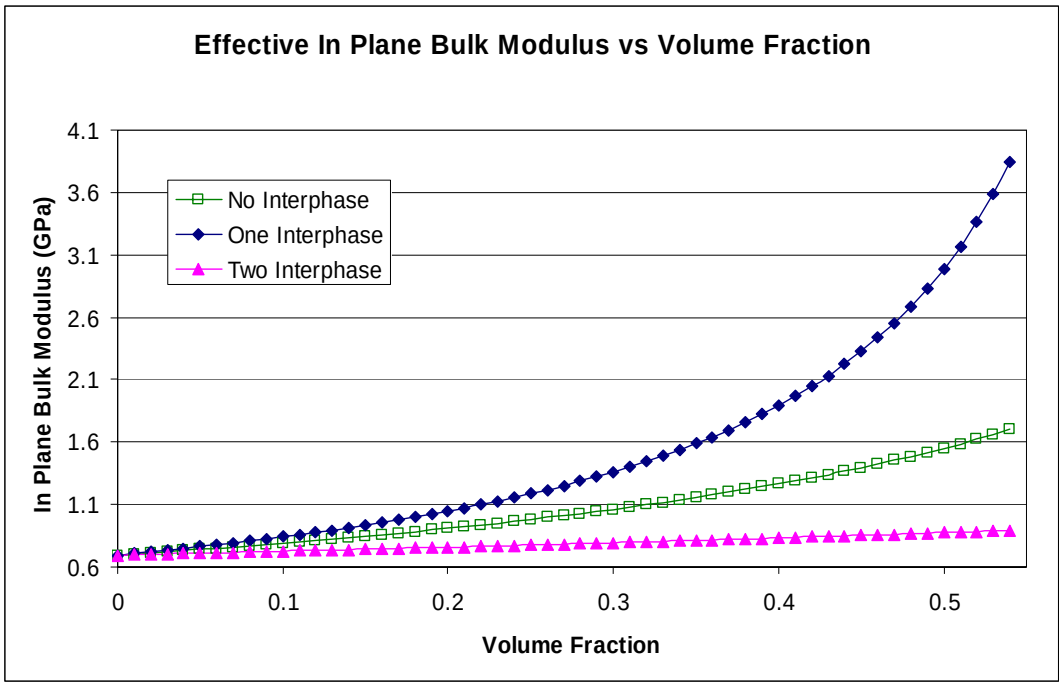

Figure 8. Multi-layered composite cylinder predictions of the effective in-plane bulk modulus of carbon nanotube reinforced polyethylene.

Figures 9 and 10 illustrate another interesting aspect of the difference between the one and two interphase results that, is the relative difference in comparison to the no interphase case at low and high volume fractions. Shown in Figure 9 are the same results as shown in Figure 8, but only up to 10% volume fraction, which is the volume fraction of the nanotube in the previously discussed molecular dynamics simulation (Figure 1) and reflective of current composite manufacturing capabilities. At such small volume fractions, it is observed that the one interphase results demonstrate less increase in effective in-plane bulk modulus relative to the no interphase results than decrease shown in the two interphase results. However, Figure 10, which illustrates the percent difference relative to the no interphase results of the one and two

interphase results up to the critical volume fraction, indicates that at higher volume fractions the increase in one interphase results becomes larger than the decrease in the two interphase results. Recall that by Equation 1, the outer radius of the matrix is decreasing with increasing volume fraction. As the matrix is less stiff than the single interphase in the one interphase case, as the volume fraction increases the influence of the interphase region's stiffness increases. In the two interphase case, both the first interphase and the matrix are less stiff than the second interphase so that as the volume fraction is increases there are competing influences on the effective properties. Increasing the volume fraction reduces the amount of matrix, but increases the influence of both interphase regions, the stiffer of which is twice the thickness of the other. This observation again leads to the conclusion that accurate representation of the interphase region is important in predicting effective properties.

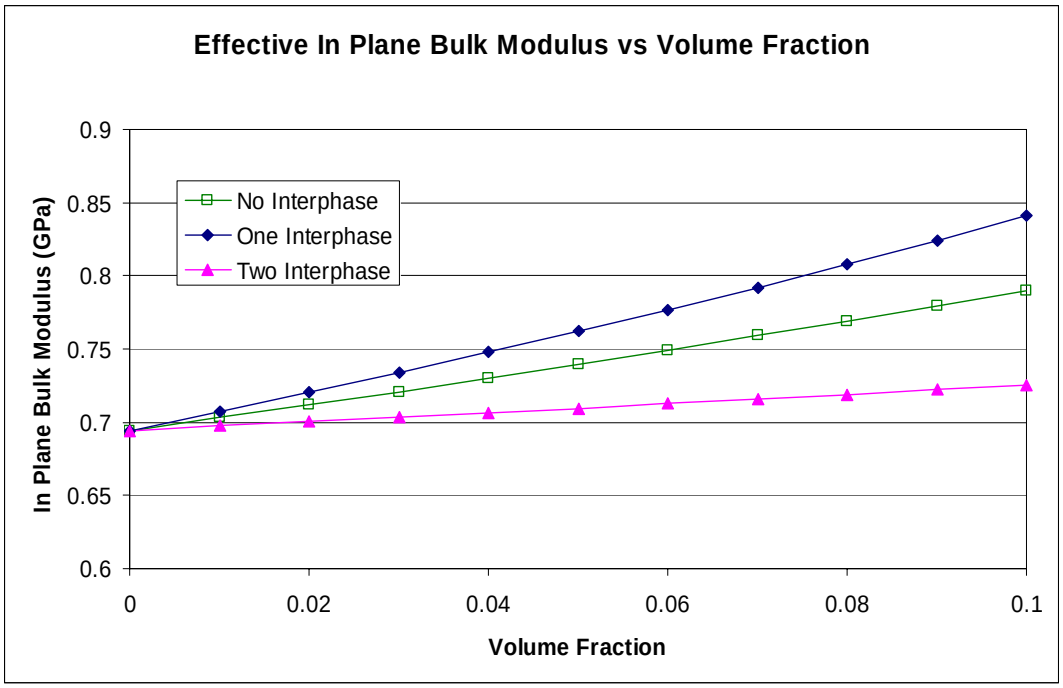

Figure 9. Multi-layered composite cylinder predictions of the effective in-plane bulk modulus of carbon nanotube reinforced polyethylene up to 10% volume fraction (the volume fraction of the previously discussed molecular dynamics simulation).

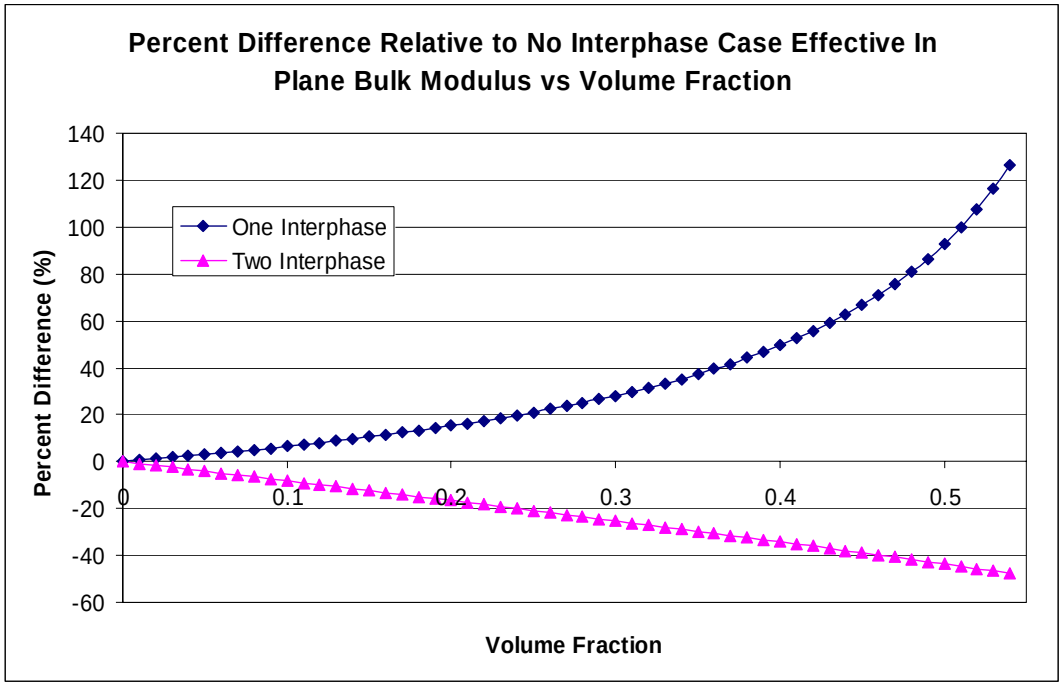

Figure 10. Percent difference relative to the no interphase case of the in-plane bulk modulus obtained for the one and two interphase cases.

SUMMARY AND CONCLUSIONS

Molecular dynamics simulations of a carbon nanotube in a polyethylene matrix have been used to obtain a radial distribution in density. This radial distribution in density has motivated the inclusion of a functionally graded interphase region into micromechanics predictions of the composite's effective elastic constants. The functionally graded interphase has been modeled on the micromechanics level using one or more piecewise continuous interphase regions in a multi-layered composite cylinder approach. It has been observed that the functional form of the interphase region has no significant effect on the effective axial modulus, but does strongly influence the effective axial Poisson's ratio, axial shear modulus and in-plane bulk modulus. It is also observed that having even one of the piecewise continuous interphase subregions with a Young's modulus less than that of the matrix can cause large reductions in the effective axial shear modulus and in-plane bulk modulus relative to the same composite with no interphase present. Given the importance of accurately representing the interphase region on the effective elastic constants indicated by using a piecewise continuous representation of the interphase, it is natural to ponder the implications of instead using say a piecewise liner representation. In such cases, as indicated in Equation 7 (where $\mathbf{L}$ is the stiffness tensor and $\boldsymbol{\varepsilon}$ the strain tensor), a second term involving the divergence of the stiffness in the equilibrium equation becomes non-zero. In addition, the large reduction in some of the effective properties due to the inclusion of the very compliant interphase also suggests that the incorporation of non-perfect interface conditions (i.e. altering the assumptions of Equation 5) may be significant. Future efforts will seek to ascertain how strongly these two assumptions may influence the effective properties.

$$\mathrm{div}\left(\mathbf{L}\right)\boldsymbol{\varepsilon}+\mathbf{L}\,\mathrm{div}\left(\boldsymbol{\varepsilon}\right)=\mathbf{0} \tag{7}$$

REFERENCES

1. S. J. V. Frankland, V. M. Harik, G. M. Odegard, D. W. Brenner and T. S. Gates. 2003. "The stress-strain behavior of polymer-nanotube composites from molecular dynamics simulation" *Composite Science and Technology*, 63, pp. 1655-1661.
2. S. J. V. Frankland, A. Caglar, D. W. Brenner and M. Griebel. 2002. "Molecular Simulation of the Influence of Chemical Cross-Links on the Shear Strength of Carbon Nanotube-Polymer Interfaces" Journal of Physical Chemistry B, 106, pp. 3046-3049.
3. G.D. Seidel and D.C. Lagoudas. 2005. "Micromechanical analysis of the effective elastic properties of carbon nanotube reinforced composites" Accepted by Mechanics of Materials.
4. D.W. Brenner, O.A. Shenderova, J.A. Harrison, S.J. Stuart, B. Ni, and S.B. Sinnott. 2002. "A second-generation reactive empirical bond order (REBO) potential energy expression for hydrocarbons" *Journal of the Physics of Condensed Matter*, 14, 783.
5. Z. Hashin and H. Rosen. 1964. "The elastic moduli of fiber-reinforced materials" *Journal of Applied Mechanics*, 31, pp. 223-232.
6. R.M. Christensen and K.H. Lo. 1979. "Solutions for effective shear properties in three phase sphere and cylinder models", 27, pp. 315-330.
7. http://www.matweb.com